



## Molecular Crystals and Liquid Crystals Incorporating Nonlinear Optics

Publication details, including instructions for authors and  
subscription information:

<http://www.tandfonline.com/loi/gmcl17>

## Small Angle Scattering From Multiphase Polymers

R. W. Richards<sup>a</sup>

<sup>a</sup> Department of Pure and Applied Chemistry, University of  
Strathclyde, Glasgow, G1 1XL, UK

Version of record first published: 22 Sep 2006.

To cite this article: R. W. Richards (1990): Small Angle Scattering From Multiphase Polymers,  
Molecular Crystals and Liquid Crystals Incorporating Nonlinear Optics, 180:1, 55-67

To link to this article: <http://dx.doi.org/10.1080/00268949008025788>

PLEASE SCROLL DOWN FOR ARTICLE

Full terms and conditions of use: <http://www.tandfonline.com/page/terms-and-conditions>

This article may be used for research, teaching, and private study purposes. Any  
substantial or systematic reproduction, redistribution, reselling, loan, sub-licensing,  
systematic supply, or distribution in any form to anyone is expressly forbidden.

The publisher does not give any warranty express or implied or make any representation  
that the contents will be complete or accurate or up to date. The accuracy of any  
instructions, formulae, and drug doses should be independently verified with primary  
sources. The publisher shall not be liable for any loss, actions, claims, proceedings,  
demand, or costs or damages whatsoever or howsoever caused arising directly or  
indirectly in connection with or arising out of the use of this material.

# Small Angle Scattering From Multiphase Polymers

R. W. RICHARDS

*Department of Pure and Applied Chemistry, University of Strathclyde, Glasgow, G1 1XL, UK*

## INTRODUCTION

Small angle neutron scattering (SANS) studies of polymers have produced much insight into the molecular and supramolecular physics of polymer systems. A considerable amount of work in this laboratory has been focussed on multiphase polymer systems. This contribution surveys some of that work and presents some data from projects which are still continuing. There are three main topics, block copolymers, interpenetrating polymer networks and block copolymer monolayers. Since the review covers a broad field it will necessarily be concise in parts, however plentiful references will be made to the original papers.

## BLOCK COPOLYMERS

### 1. Styrene-Isoprene Block Copolymers in the Solid State

Almost from their original synthesis the special aspects of the solid state structure of styrene-diene block copolymers were recognised from electron microscopy investigations.<sup>1</sup> Since the polystyrene and polyisoprene blocks are thermodynamically incompatible, they phase separate at temperatures below a critical value depending on molecular weight, however, due to the molecular connectivity of the two chemically distinct sequences, this demixing is a microphase separation process with domains of regular morphology of the minor component being dispersed through a matrix of the major constituent of the block copolymer. Molau was perhaps the first to identify particular domain morphologies with specific composition ranges.<sup>2</sup> For example in styrene-diene diblock copolymers, for weight fractions of polystyrene (PS) up to circa 0.2, spherical PS domains are obtained, for weight fractions between 0.2 to 0.4 cylindrical PS domains prevail, and for weight fractions between

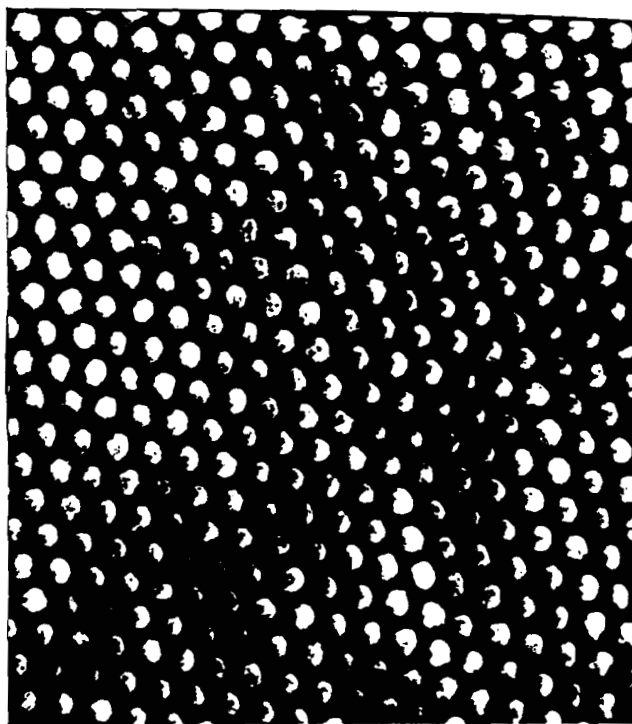


FIGURE 1 Electron micrograph of styrene-isoprene linear diblock copolymer with a styrene weight fraction of 0.25.

0.4 and 0.6 on alternating lamellar structure is seen. Furthermore, as the electron micrograph of Figure 1 shows the domains have considerable long range order. Meier<sup>3</sup> was the first to produce a statistical thermodynamic description of block copolymer structure. Subsequently, Helfand<sup>4</sup> and Leibler<sup>5</sup> have also produced theories. Perhaps that due to Helfand is the most complete in that values of domain size, separation and their dependence on molecular weight may be calculated. Consequently a test of the theory requires values of the quantities listed above.

Typically domain dimensions (radius or half thickness) are circa 100 Å whilst separations are around 500 Å. These length scales mean that a small angle radiation scattering law will contain contributions from isolated domains (single particle form factor) and an interference function due to the regular arrangement of domains.<sup>6</sup> An additional contribution arises from the diffuseness of the boundary between matrix and domain due to entropic fluctuations in the random walk for each block whereby short runs of each component protrude into the domain space of the other component. This results in a smooth change in density from one phase to the other and it may be described by a Gaussian function. Combining these aspects together produces the total scattering law.

$$S^T(Q) = (\rho_p - \rho_m)^2 \langle F_p(Q) \rangle^2 A(Q) \exp(-\sigma^2 Q^2) + \Sigma_i / 4\pi \quad (1)$$

where

- $Q$  = scattering vector =  $4\pi/\lambda \sin \theta$  ( $2\theta$  = scattering angle)  
 $\langle F_p(Q) \rangle^2$  = single particle form factor for an isolated domain  
 $A(Q)$  = interference function  
 $\sigma^2$  = mean square standard deviation of the segment density distribution across the interface  
 $\Sigma_i/4\pi$  = incoherent background scattering  
 $(\rho_p - \rho_m)^2$  = contrast factor where  $\rho_p$  and  $\rho_m$  are the coherent scattering length densities of the domain and matrix respectively.

Figure 2 clearly shows the contribution of the interference function by the sharp Bragg peaks evident at very low  $Q$  values, at higher  $Q$  values the broad maxima arise from the single particle form factor scattering of the cylindrical polystyrene domains in this case. The solid line through these latter points is the fit of the scattering law for an isolated cylinder adjusted for a distribution in cylinder radius and a distribution of cylinder orientation with respect to the  $Q$  vector. Values of domain dimensions as a function of the molecular weight of the domain forming block and the comparison with the predictions of the Helfand theory are shown in Figure 3.<sup>7</sup> In general the agreement is good. The interdomain separation obtained by SANS does not have such good agreement with the Helfand predictions, the absolute values of the separation differs somewhat, additionally different scaling exponents with molecular weight are observed. This is probably due to the kinetic restrictions (viscosity increase) preventing further movement in the domains at some stage during sample preparation, i.e. the domains have a non-equilibrium separation.

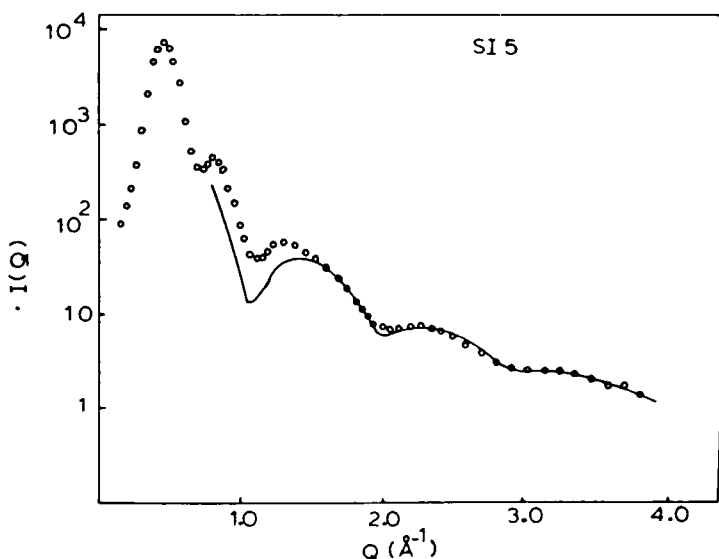


FIGURE 2 Small angle neutron scattering profile from a triblock styrene-isoprene-styrene copolymer. Solid line is a fit of the single particle form factor for a cylinder of radius 120 Å.

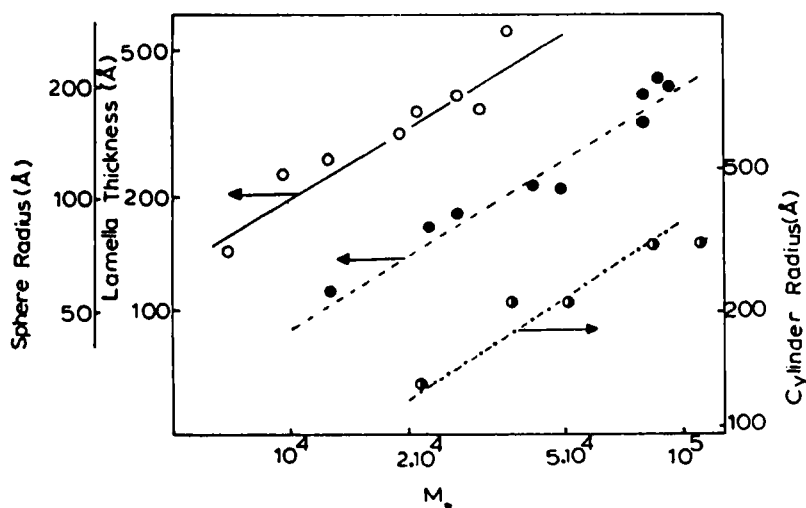


FIGURE 3 Domain dimensions for spherical, (—) cylindrical (— — —) and lamellar (— · —) domains.

The interference function has been modelled by using an expression for a one dimensional 'macrocrystallin' lattice and then investigating the influence of the individual parameters on the resultant scattering.<sup>8</sup> A typical fit of calculated and experimental data is shown in Figure 4. The distortions to the expression needed to produce this agreement correspond to the domains being on a *paracrystalline* lattice.

The existence of a diffuse domain-matrix interface was remarked on earlier.

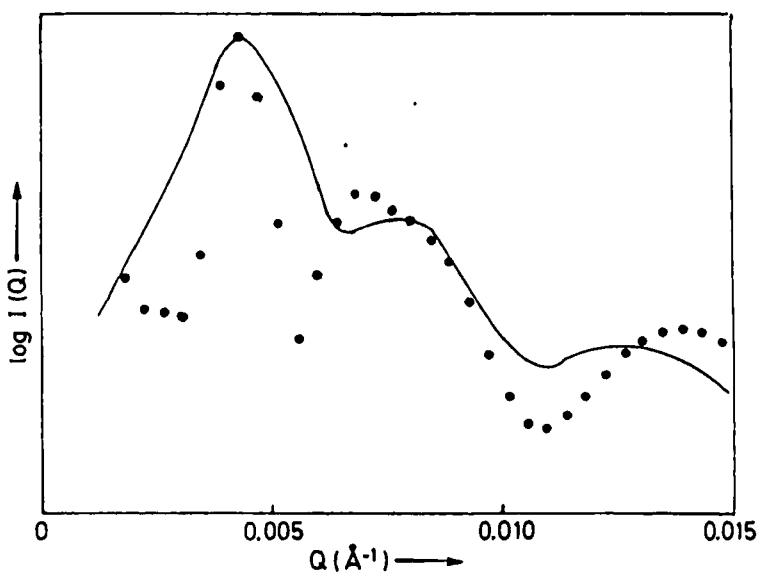
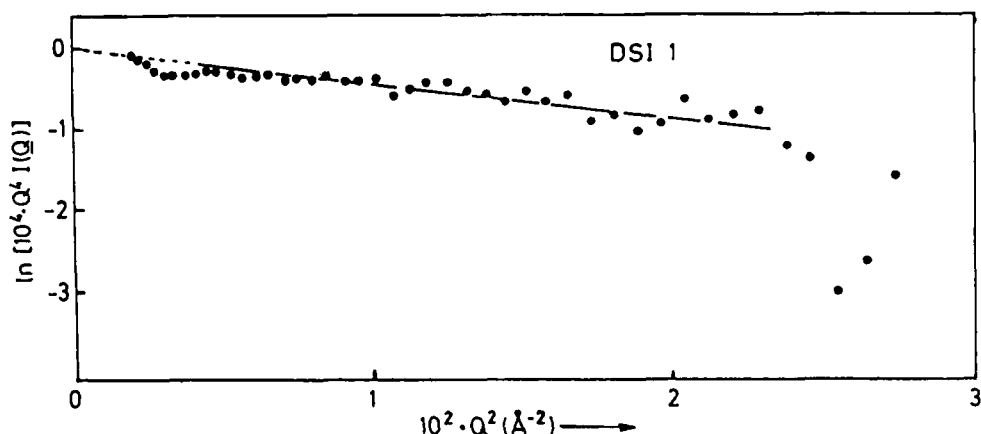


FIGURE 4 Calculated interference function scattering (●) compared to experimental data (-).

FIGURE 5 Plot of data according to equation 2 for evaluation of  $\sigma$ .

Estimation of the thickness of this diffuse interface depends on negative deviations from Porods law which states that at sufficiently high  $Q$  values then  $I(Q) \propto Q^{-4}$ . In the presence of a diffuse interface and after *accurate* subtraction of the incoherent background scattering then

$$\ln(Q^4 I(Q)) = \ln K^* - \sigma^2 Q^2 \quad (2)$$

where  $K^*$  contains calibration factors and the surface (area) to volume ratio of the scattering particle. Figure 5 shows data for a deuterostyrene-isoprene copolymer plotted according to Equation 2 with a least squares line through the linear portion.<sup>9</sup> From the value of the  $\sigma$  obtained from the slope, the diffuse layer thickness can be obtained since  $t = \sqrt{12} \sigma$ . The volume fraction of the interfacial region calculated from values of  $t$  are shown as a function of copolymer molecular weight in Figure 6, again the Helfand theory appears to give the better agreement.

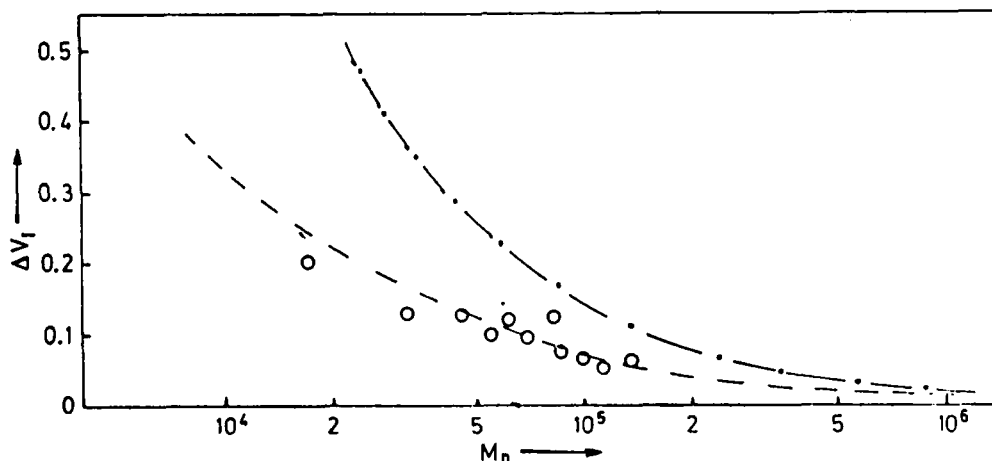


FIGURE 6 Interfacial volume fraction as a function of copolymer molecular weight.

## 2. Phase Separation Kinetics

There has been much interest in the kinetics of phase separation of polymer blends. Light, X-ray and neutron scattering have been used to evaluate kinetic parameters usually by using the linear Cahn-Hilliard<sup>10</sup> theory. Attention to block copolymer phase separation kinetics has been much less. The thermodynamics of the transformation of a linear diblock block copolymer from a high temperature homogenous disordered phase to a lower temperature ordered (microphase separated) phase were set out using the random phase approximation by Leibler.<sup>5</sup> Such calculations have been repeated and extended to other copolymer architectures using projection operator methods by Sanchez and co-workers.<sup>11</sup> In particular the scattering law for the homogenous state has been written down and this has a maximum at a finite  $Q$  value in contrast to a homogenous blend of two homopolymers where the maximum scattered intensity is at  $Q = 0$ . As temperature is reduced this maximum grows in amplitude since its shape is controlled by the value of  $\chi$ , the Flory-Huggins interaction parameter between the two component polymers which make up the copolymer. If a copolymer in the homogenous state is suddenly quenched to a lower temperature then the intensity will change with time as the system relaxes to its new equilibrium state according to the equation.<sup>12</sup>

$$I(Q, t) = I(Q, 0) \exp (2R(Q)t) \quad (3)$$

where  $R(Q)$  is effectively the first order rate constant for the relaxation process and

$$R(Q) = L_o Q^2 (-(F(U)/N) - 2\chi) \quad (4)$$

with  $F(U)$  = A composition weighted sum of Debye expressions for the scattering from individual polymer chains

$N$  = Degree of polymerisation of the copolymer

$L_o$  = Onsager coefficient connecting the diffusive flux of molecules to the local chemical potential

Now as the system goes into the microphase separated region the intensity as given by the random phase expressions and equation 3 becomes discontinuous since a critical value of the product  $N\chi$  is crossed. However, the variation of  $R(Q)$  with time is continuous and may still be evaluated from a series of time resolved small angle scattering experiments no matter how deep the quench from the homogeneous state. We have recently completed a series of SANS experiments investigating these aspects of block copolymer phase separation using very concentrated solutions of polydeuterostyrene-polyisoprene block copolymers in cyclohexane solution.<sup>13</sup> The cyclohexane was composed of hydrogenous and deuterio isotopes so that the scattering length density matched that of the polyisoprene blocks, consequently only the polydeuterostyrene portion was the source of the scattering signal. The presence of the solvent aids the flow of heat from the relatively thick (1mm) specimens on quenching. SANS measurements were made as a function of temperature using a block copolymer with a weight fraction of polystyrene of 0.19, some of the scattering profiles are shown in Figure 7. At the lowest temperature

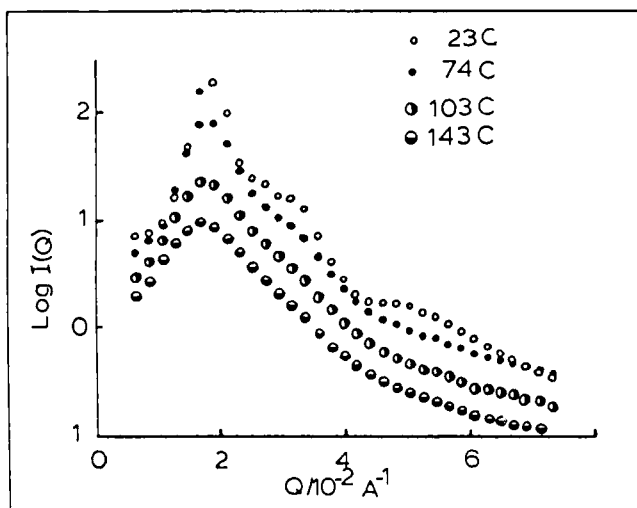


FIGURE 7 Scattered neutron intensity for a linear deuterio-styrene-isoprene diblock copolymer ( $W_s = 0.19$ ) in a 70% cyclohexane solution as a function of temperature.

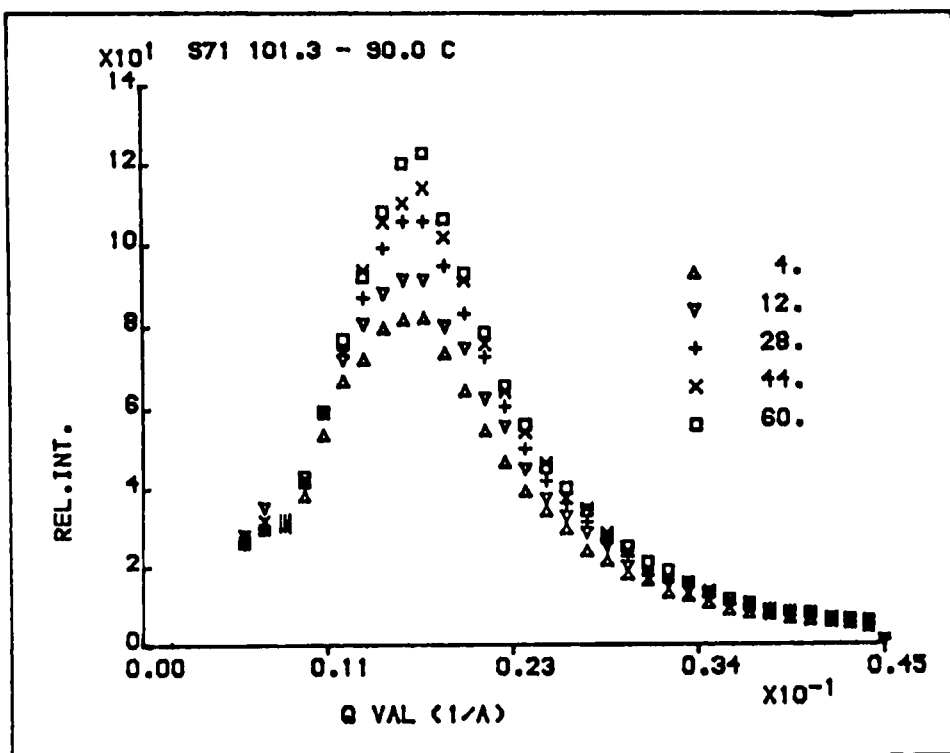


FIGURE 8 Evolution of scattered intensity as a function of time after quenching from 101.3°C to 90°C for the same system as in Figure 7.



an ordered microphase structure is evident, whilst at the highest temperature only the broad maximum characteristic of the random phase description of the scattering is evident. The transition temperature is easily identified from a plot of (maximum intensity) $^{-1}$  as a function of (temperature) $^{-1}$ . Values of the radius of gyration of the copolymer and  $\chi$  were obtained from fitting the random phase expressions to the data, in all cases the fit was good for copolymers in the homogeneous phase. For time resolved scattering, specimens were equilibrated at temperatures well in the homogeneous range and then suddenly dropped into a lower thermostated jacket mounted in the beam. Data were collected for a series of discrete time frames, each frame of duration 2s to 8s, for total times of up to 300 seconds. To acquire sufficient statistical accuracy it was necessary to repeat this process at least 10 times. Figure 8 shows the evolution of scattered intensity as a function of time for one quench depth. For each  $Q$  value, the intensity data was plotted according to equation 3 and  $R(Q)$  extracted from the slope. A plot of  $R(Q)/Q^2$  as a function of  $Q^2$  is shown in Figure 9 where the solid line is the fit of Equation 4, fitting parameters being radius of gyration,  $\chi$  and  $L_o$ . The values of the first two parameters are average values over the temperature range traversed during quenching. From the values of  $L_o$  obtained the growth rate of the concentration fluctuations of various

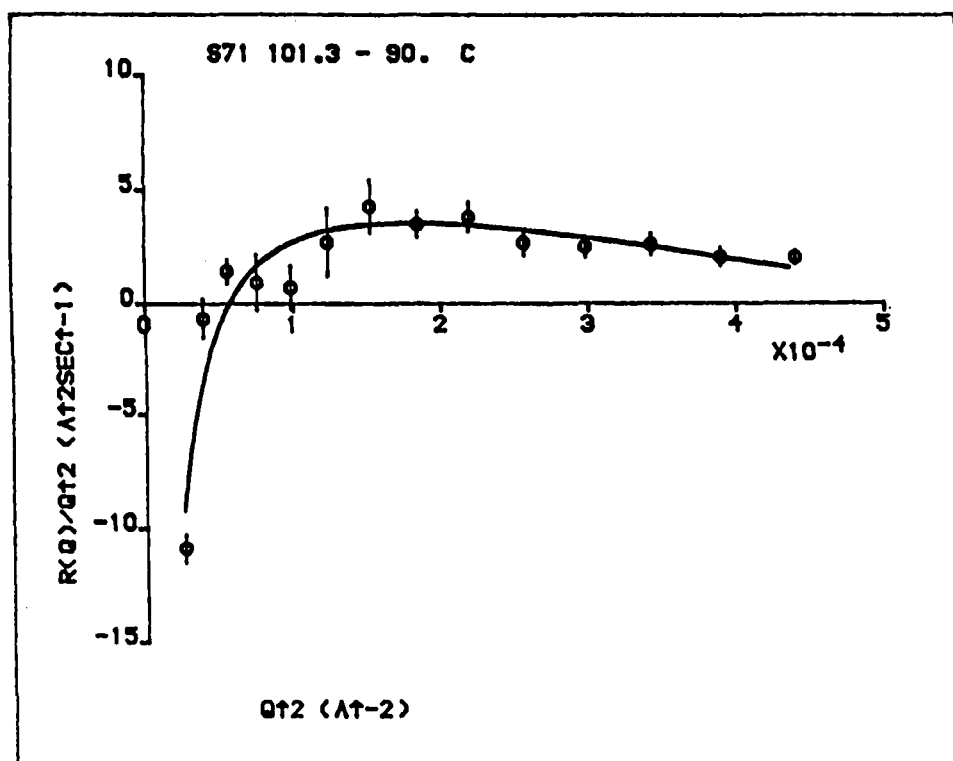


FIGURE 9  $R(Q)/Q^2$  as a function of  $Q^2$  for a quench from 101.3°C to 90°C for the system of Figure 7.

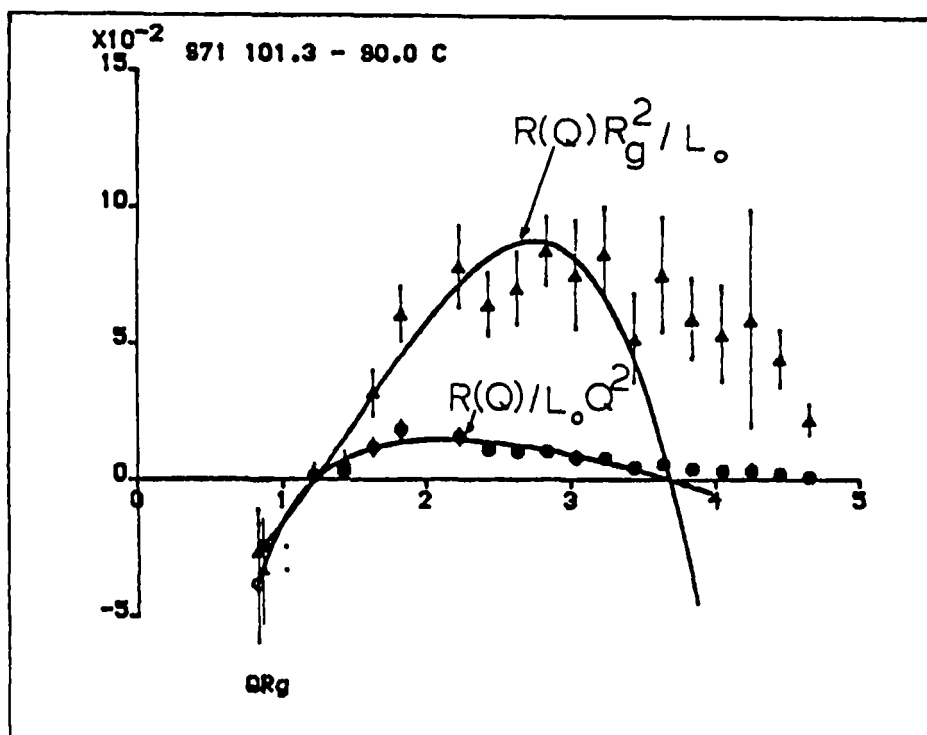


FIGURE 10 Growth rate of density fluctuations and local thermodynamic drifting force as a function of  $Q$ .

wavelength can be obtained as well as the local thermodynamic driving force (Figure 10). The growth rate certainly shows the maximum at a finite  $Q$  value and the lower critical  $Q$  value below which phase growth is not promoted, both of these being predicted by the theory. However, no upper critical  $Q$  value for phase growth limitation is evident, this is thought to be due to the neglect of thermal fluctuations in the expression for the scattering and the simplified  $Q$  independent Onsager coefficient used.

### Interpenetrating Polymer Networks (IPNs)

IPN materials are produced when a monomer is polymerised and crosslinked whilst in intimate contact with a preformed network of a different polymer. They are generally phase separated and predictions of phase separated zone size based on Flory-Huggins theory have been produced by Yeo et al<sup>14</sup> on the basis of isolated spherical regions. SANS data on IPNs consisting of deuterio-polystyrene (PSD) guest polymer<sup>15</sup> in a polydimethyl siloxane (PDMS) network<sup>16</sup> is featureless showing a smooth decrease with increasing  $Q$ . A priori, there is no reason to suspect that the PSD zones, especially at high PSD content, should be spherical. Fortunately, electron micrographs for this system indicated that the zones were spherical. SANS data were analysed in two ways using Porod law analysis to evaluate an

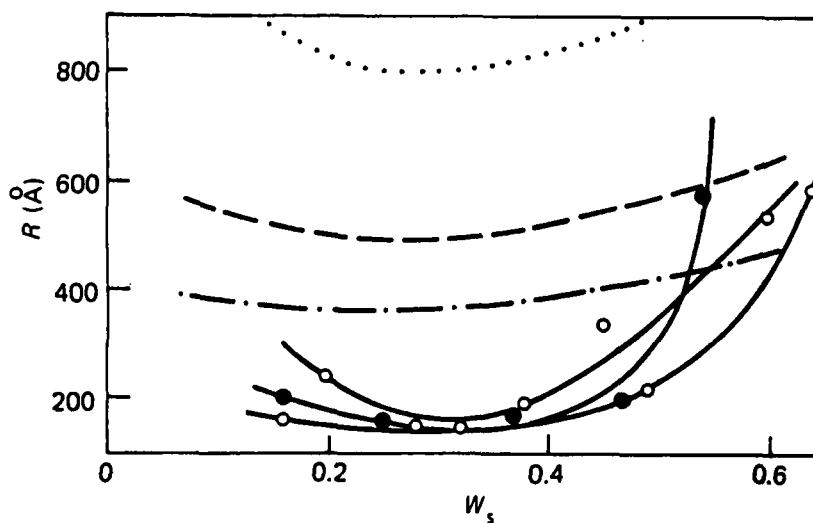


FIGURE 11 Radii of phase separated polystyrene zones in polydimethyl siloxane/polystyrene interpenetrating networks as a function of weight fraction of polystyrene.

equivalent sphere radius and using the statistical description of scattering and evaluating the correlation function. The radii obtained by the first approach are shown in Figure 11 which includes the predictions of the Yeo theory for PDMS networks with three differing crosslink densities. From the correlation functions, the mean chord length in the PSD phase was calculated and these show a similar

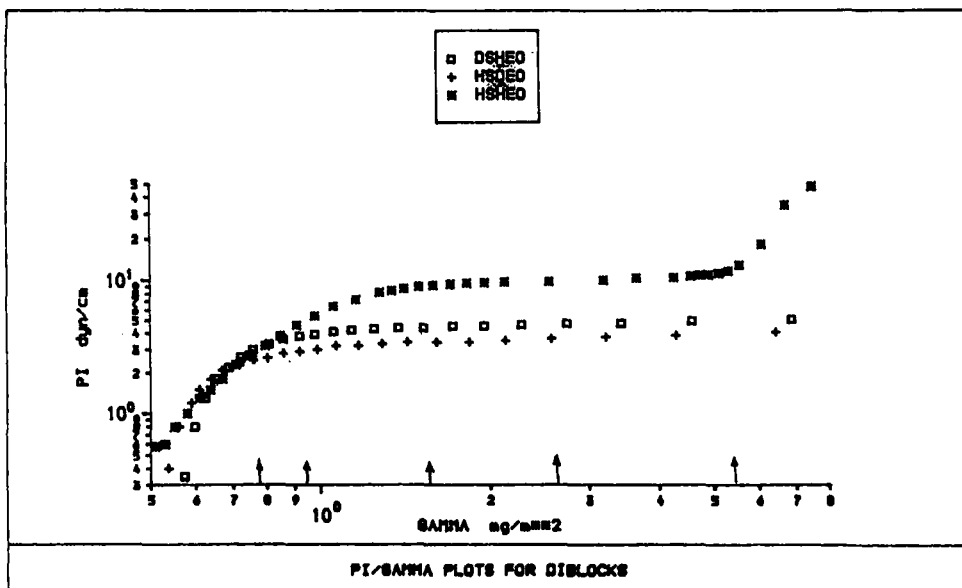


FIGURE 12 Variation of surface pressure with surface concentration for a monolayer of a styrene-ethylene oxide block copolymer spread at the air/water interface.

shaped dependence on IPN composition as the equivalent sphere radii. It is clear, however, that the absolute magnitude of the theoretical predictions are in poor agreement with experiment.

## BLOCK COPOLYMER MONOLAYERS

In collaboration with Dr. R. K. Thomas at Oxford University, we have recently begun a neutron reflectometry study of styrene-ethylene oxide diblock copolymers spread at the air/water interface. These experiments were made using the CRISP reflectometer at the pulsed neutron source, ISIS, in the UK. Figure 12 shows the surface pressure variation with surface concentration for some of the block copolymers investigated. The neutron reflection profile for a completely hydrogenous copolymer on a D<sub>2</sub>O surface is shown in Figure 13, the solid line being the fit of a solid slab to the data. A selection of the polyethylene oxide layer thickness and compositions as a function of surface concentration is shown in Table 1. Overall these first data suggest that the polystyrene layer has a constant thickness but contains water. As the surface concentration increases this water is rejected from the styrene. At the same time the polyethylene oxide layer which is partially solvated becomes more dilute and extends further into the subphase. Using a kinematic description<sup>17</sup> of the neutron reflectivity ( $R(Q)$ ) we can write;

$$\ln Q^4 R(Q) = 16\pi^2 \Delta\rho - \sigma^2 Q^2$$

where  $\Delta\rho$  is the difference in scattering length density for a sharp interface and  $\sigma$  the standard deviation of the scattering length density distribution. Data are plotted

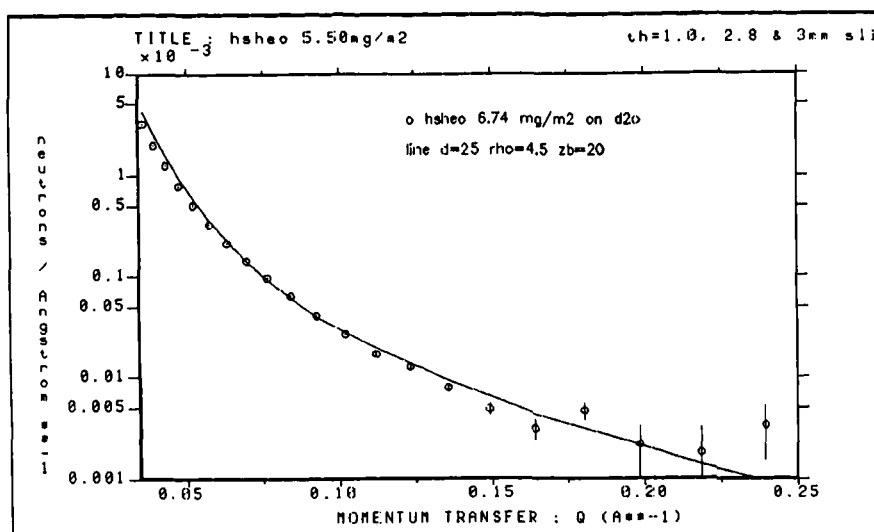


FIGURE 13 Neutron reflectivity as a function of  $Q$  for a fully hydrogenous styrene-ethylene oxide block copolymer spread at the air/water interface.

TABLE I  
Layer thickness (*t*) calculated from fits to reflectivity profiles from a hydrogenous styrene-ethylene oxide block copolymer spread at the air/water interface.

Surface Concentration/mg m <sup>-2</sup>	<i>t</i> /Å
0.77	20
1.53	24
2.6	28
5.49	42

according to this equation in Figure 14 whilst Table 2 shows the values of the thickness, *t*, of the diffuse boundary layer (i.e. solvated polyethylene oxide) calculated from the relation  $t = \sqrt{12\sigma}$ .

CONCLUSIONS

Aspects not mentioned here include association of block copolymers in dilute solution<sup>18</sup> and deformation induced changes in supramolecular structure,<sup>19</sup> both of which have been studied in this laboratory. Work in progress includes studies of main chain liquid crystal polymers, semi-crystalline block copolymers and molecular deformation of triblock copolymers. A complete application of SANS to the many facets of polymer science is still a long way in the future.

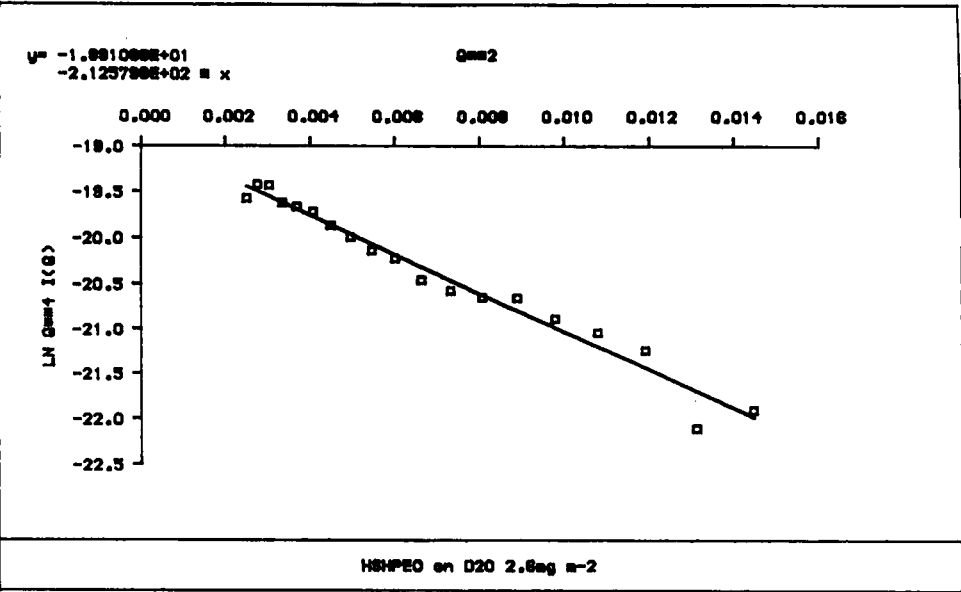


FIGURE 14 Reflectivity data plotted in Porod equation form.

## References

1. See for example "Block Polymers" ed. S. L. Aggarwal, Plenum Press, N.Y., 1970.
2. G. Molau, p. 79 in Reference 1.
3. D. J. Meier, *J. Polym. Sci.*, **C26**, 81 (1969).
4. E. Helfand in "Developments in Block Copolymers—1" ed. I. Goodman, Applied Science Publishers, 1982.
5. L. Leibler, *Macromolecules*, **13**, 1602 (1980).
6. R. W. Richards and J. L. Thomason, *Polymer*, **24**, 581 (1981).
7. R. W. Richards and J. L. Thomason, *Macromolecules*, **16**, 982 (1983).
8. R. W. Richards and J. L. Thomason, *Macromolecules*, **18**, 452 (1985).
9. R. W. Richards and J. L. Thomason, *Polymer*, **24**, 1089 (1983).
10. K. Binder, *Coll. Polym. Sci.*, **265**, 273 (1987).
11. M. Olvera de la Cruz and I. Sanchez, *Macromolecules*, **19**, 1621 (1986).
12. T. Hashimoto, *Macromolecules*, **20** (1987).
13. J. G. Connell and R. W. Richards in "Polymer Motion in Dense Systems," Springer. To be published.
14. J. K. Yeo, L. H. Sperling and D. A. Thomas, *Polymer*, **24**, 307 (1983).
15. B. McGarey and R. W. Richards, *Polymer*, **27**, 1315 (1987).
16. B. McGarey and R. W. Richards, *Br. Polym. J.*, **19**, 111 (1987).
17. T. L. Crowley, R. K. Thomas and A. Willat, To be published.
18. C. J. C. Edwards, R. W. Richards and R. F. T. Stepto, *Polymer*, **27**, 643 (1986).
19. J. T. Mullin and R. W. Richards, *Symp. Proc. Mat. Res. Soc.*, **79**, 299 (1987).